Lasers in Medical Science
https://doi.org/10.1007/s10103-018-2677-4

ORIGINAL ARTICLE

The antifungal agent of silver nanoparticles activated by diode laser as light source to reduce *C. albicans* biofilms: an in vitro study

Suryani D. Astuti[1,2] · Putri S. Puspita[3] · Alfian P. Putra[4] · Andi H. Zaidan[1] · Mochamad Z. Fahmi[5] · Ardiyansyah Syahrom[6,7] · Suhariningsih[1]

Received: 21 May 2018 / Accepted: 30 October 2018

Abstract

Candida albicans is a normal flora caused fungal infections and has the ability to form biofilms. The aim of this study was to improve the antifungal effect of silver nanoparticles (AgNPs) and the light source for reducing the biofilm survival of *C. albicans*. AgNPs were prepared by silver nitrate ($AgNO_3$) and trisodium citrate ($Na_3C_6H_5O_7$). To determine the antifungal effect of treatments on *C. albicans* biofilm, samples were distributed into four groups; L + P+ was treatment with laser irradiation and AgNPs; L + P− was treatment with laser irradiation only; L − P+ was treatment with AgNPs only (control positive); L − P− was no treatment with laser irradiation or AgNPs (control negative). The growth of fungi had been monitored by measuring the optical density at 405 nm with ELISA reader. The particle size of AgNPs was measured by using (particle size analyzer) and the zeta potential of AgNPs was measured by using Malvern zetasizer. The PSA test showed that the particle size of AgNPs was distributed between 7.531–5559.644 nm. The zeta potentials were found lower than − 30 mV with pH of 7, 9 or 11. The reduction percentage was analyzed by ANOVA test. The highest reduction difference was given at a lower level irradiation because irradiation with a density energy of 6.13 ± 0.002 J/cm^2 resulted in the biofilm reduction of 7.07 ± 0.23% for the sample without AgNPs compared to the sample with AgNPs that increased the biofilm reduction of 64.48 ± 0.07%. The irradiation with a 450-nm light source had a significant fungicidal effect on *C. albicans* biofilm. The combination of light source and AgNPs provides an increase of biofilm reduction compared to the light source itself.

Keywords AgNPs · Lasers diode · *Candida albicans* · Antifungal effect · Biofilm

✉ Suryani D. Astuti
suryanidyah@fst.unair.ac.id

[1] Department of Physics, Faculty Science and Technology, Universitas Airlangga, Surabaya 60115, Indonesia

[2] Biomedical Engineering Master Program, Post Graduate School, Universitas Airlangga, Surabaya 60115, Indonesia

[3] Magister of Physics Engineering, Institute of Technology Sepuluh Nopember, Surabaya 60111, Indonesia

[4] Biomedical Engineering Study Program, Department of Physics, Faculty of Sciences and Technology, Universitas Airlangga, Surabaya 60115, Indonesia

[5] Department of Chemistry, Faculty of Sciences and Technology, Universitas Airlangga, Surabaya 60115, Indonesia

[6] Department of Applied Mechanics and Design, Faculty of Mechanical Engineering, Universiti Teknologi Malaysia, 81310 Johor Bahru, Malaysia

[7] Sports Innovation and Technology Centre (SITC), Institute of Human Centred and Engineering (IHCE), Universiti Teknologi Malaysia, 81310 Johor Bahru, Malaysia

Introduction

Invasive candidiasis (IC) is a form of serious infection caused by the fungal species called *Candida albicans* (*C. albicans*). The infection manifests on several matters, such as candidemia, disseminated candidiasis, endocarditis, meningitis, and endophthalmitis. A previous report related to IC in some countries shows that the infections caused by fungal are still high and tend to increase every year [1–3]. Other studies on IC case reported with a similar problem such as high mortality rate, needing a long-term treatment, and being costly [4–6]. Moreover, one of the difficulties of these treatments is the characteristic of *C. albicans* being resistance to antifungal drugs, including amphotericin B, nystatin, clotrimazole, and fluconazole. Drug susceptibility studies have revealed that biofilms of *C. albicans* are up to 2000 times more resistant compared to planktonic cells [7, 8]. This resistance occurs by layer protector is called extracellular polymeric substance (EPS). EPS biofilm of mature *C. albicans* has a

Published online: 09 November 2018

complex three-dimensional structure consisting of solid tissue of yeast, hyphae, and pseudohyphae included in a matrix of extracellular material. The β-1,3-glucan within the *C. albicans* biofilm matrix plays an important role in the biofilm-mediated protection of *C. albicans* from immune defenses and antifungals. The production of β-1,3-glucan by *C. albicans* biofilms inhibits the production of reactive oxygen species (ROS) and protects fungal cells [9].

Particles in the nano-range have unique physical and chemical properties and useful materials in biological applications such as medicines, antimicrobial agents, wound dressing, drug targeting and deliveries, transfection vectors, bioimaging, and labeling agents [10]. Silver nanoparticles (AgNPs) have attracted significant attention and interest for their potential applications in biomedicine as well as antibacterial devices. Silver is an effective antimicrobial agent can inhibit pathogenic microorganisms such as viruses, bacteria, fungi, and eukaryotic microorganisms in the low concentrations. Rahisuddin et al. showed antimicrobial and antifungal planktonic effect of silver nanoparticles in the low concentration (microgram per milliliter) [11]. Rahisuddin said that the mechanism of inhibitory action of silver ions on microorganisms has been established due to the electrostatic interaction with the DNA, cellular proteins, sulfur-containing (especially thiol group) functional groups of respiratory enzymes or proteins, negatively charged bacterial cells, and building elements of the bacterial membrane. Thiol group (–SH) possess high affinities towards silver ions and assumed that inhibitory action might be due to the reduction of the SH cell membrane by AgNPs [11]. The adhesion of *Candida* cells was significantly reduced, mainly when biofilms were pretreated with 54 μg/mL AgNPs [12]. *C. albicans* biofilms can be inactivated by 90% at concentrations of AgNPs higher than 108 μg/mL. The size of AgNP particles or its type did not affect the antifungal activity against *Candida* biofilm [13]. According to Silva, AgNPs had a significantly greater effect on reducing *C. glabrata* biofilm biomass compared with *C. albicans* [14]. The AgNP toxicity has also been associated with ion release, generation of ROS, and induction of oxidative stress [15].

The combination of light and photosensitizer on photodynamic therapy (PDT) produces radical oxygen species that provide antimicrobial and antifungal effects. Several PDT-based researches were reported to against *C. albicans* biofilm using organic Ps such as chlorophyll, methylene blue, toluidine blue, malachite green, allyl isothiocyanate (AITC), and methanol extracts [16–19]. The organic Ps has a microsize particle leading to difficult penetration into biofilm caused by EPS matrix. Consequently, the potential of materials to reduce the biofilm cannot be effective. The effective pore size of the biofilm was 50 nm for the loose flocs, but decreased below 10 nm for the dense biofilms; therefore, particles in the nano-size are the best choice to be used on biofilm treatment [20].

The development of light treatment combined with AgNPs against *C. albicans* biofilm was still being explored. The treatment of light source against *C. albicans* planktonic has been done by Imamura et al. which indicates the possibility that laser irradiation as an effective way for eliminating fungi as well as bacteria [21]. However, in the biofilm phase, treatment with a light source is more effective on the top surface of biofilm. The *C. albicans* cells mostly in the under cover of biofilm will be not be affected. Using a visible light laser, though has limited penetration depth, photothermal therapy (PTT) shows great heating effect due to surface plasmon resonance (SPR) effect. Several studies have been conducted to apply PTT mediated by metal nanoparticle with a light energy source from visible light laser [22, 23]. Kojic et al. (2012) reported that the gold nanoparticle heating-mediated laser treatment could maintain the morphology of tissue and give bactericidal effect [23]. The aim of this study is to analyze effectiveness between AgNPs and light source to reduce *C. albicans* biofilm growths.

Materials and methods

Synthesis of silver nanoparticles

The AgNPs were prepared by a chemical reducing method. Experimentally, 150 mL of 10^{-3} M silver nitrate ($AgNO_3$) (Merck, Germany) was boiled using hot plate magnetic stirrer and added with 15 mL of 1% trisodium citrate ($Na_3C_6H_5O_7$) (Merck, Germany). During this process, the solution was mixed until we got a homogeneous solution and the color change to yellowish brown. Then, it was removed from the heating element and stirred until ambient temperature [14, 24]. The optical properties of AgNP solution were evaluated with UV-vis spectrometer (Thermo Scientific, UK) at a wavelength range of 300–1100 nm. The absorption of metal nanoparticles is due to surface plasmon resonance (SPR). Furthermore, the size distributions of AgNPs were characterized by particle size analyzer (PSA) (Malvern, USA) based on the principle of dynamic light scattering. For changes, the pH values of AgNPs have used HCL (pH < 7) and NaOH (pH > 7) solutions. The AgNPs was also characterized by high-resolution transmission electron microscope (TEM) at a voltage of 120 kV in a Hitachi HT7700 to observe the shape and size of the AgNPs.

Cytotoxicity test

A monolayer of human hepatocyte cells was grown (at 37 °C in 48 h) in Dulbecco's modified Eagle's medium (D-MEM) supplemented with 5% fetal bovine serum (FBS). The culture cells were washed 5 times using phosphate-buffered saline (PBS) and trypsin versene was added to release the cell from

the tube wall. The cell concentration was adjusted to 2×10^5 cells/mL with 100 μL fresh media (86% D-MEM, 1% penicillin/streptomycin (P/S), 100 U/mL fungizone) and then transferred to a 96-microtiter plate for incubation 24 h at 37 °C. The 5 mg/mL MTT was diluted in PBS and 10 μL of it was added to each well and incubated for 4 h at 37 °C. The 50 μL DMSO solution was added in each well and centrifuged at 30 rpm for 5 min. The result was detected by measuring its OD (%T) at microplate with enzyme-linked immunosorbent assay (ELISA) reader [25].

C. albicans biofilm culture

The samples of *C. albicans* were obtained from Laboratory of Microbiology, Faculty of Dentistry, Universitas Airlangga, Indonesia. The biofilms of *C. albicans* were studied in polystyrene microplates using the in vitro biofilm model. *C. albicans* was reactivated in Sabouraud dextrose agar (SDA) media (Oxoid, UK) incubation for one night at 37 °C before the experiment. One dose of a culture was inoculated into 10 mL of sterile physiological solution (0.85% sodium chloride (NaCl)) and homogenized for a concentration of 0.5 McFarland (107 CFU/mL), followed by a 1:20 dilution in Sabouraud dextrose broth (SDB) (Oxoid, UK) containing 8% glucose. Then, 100 μL of the suspension was transferred to each well and incubated at 37 °C for 48 h. Biofilms were grown on a well plate and washed twice with phosphate-buffered saline (PBS) (pH 7.0) to remove the adherent cells. Biofilm production was detected by measuring its OD (%T) at microplate with an ELISA reader ($\lambda = 405$ nm) [26].

Light source for in vitro treatment

The light source used was computer numerical control (CNC) laser diode instrument with a microcontroller for controlling the position of the sample holder during treatment. Laser diode had an output wavelength of 450.00 ± 22.34 nm, an output power of 53.16 ± 0.01 mW, and a laser spot size of 0.13 ± 0.03 cm^2 at 3 cm of distance irradiation. The laser spot size was according to the well area of the 96-microwell plate. Those data were from calibration result using Jasco monochromator CT-10 and Optical Power Meter (OPM) Thorlabs PM100D with range power detection PW 100–200 W and a wavelength of 185 nm–25 μm. The energy densities of 6.13 J/cm^2, 12.27 J/cm^2, 36.80 J/cm^2, 122.68 J/cm^2, 245.35 J/cm^2, and 490.71 J/cm^2 were used in this treatment. The experimental setup and the flowchart of this study was shown in Fig. 1.

Sample treatments

Surface zeta potentials were measured using Malvern zetasizer. The pH was adjusted to the required value (pH 3, 7, 9, and 11) using 1 M HCl and 1 M NaOH. Each sample was then mechanically stirred for 15 min to reach the ionic equilibrium. After shaking, the equilibrium pH was recorded and the zeta potential of the metallic particles was measured. Using the standard *C. albicans* suspension, we used two treatments following the groups to reduce biofilm (Table 1).

Treatments were divided into the following experimental groups: L + P+ was the treatment with laser irradiation and AgNPs; L + P− was the treatment with laser irradiation only; L − P+ was the treatment with AgNPs only (control positive); L − P− was no treatment with laser irradiation or AgNPs (control negative). According to the experimental groups described, 0.1 mL of the *C. albicans* suspension was added to each well of sterile 96-well flat-bottom microtiter plates with lids. After biofilm growth, 100 μL of the AgNPs was added for groups L + P+ and L − P+. The plates were shaken for 5 min in an orbital shaker. The well content of the plates of groups L + P+ and L + P− was then irradiated according to the protocol described. The irradiation was done completely in the dark room at laminar airflow. The growth of fungi in the culture had been monitored by measuring the optical density (OD) at 405 nm. Then, the antifungal effect was calculated by the following (Eq. (1)).

$$\%\text{biofilm reduction} = \left| \frac{OD_{\text{control}} - OD_{\text{treatment}}}{OD_{\text{control}}} \right| \times 100\% \quad (1)$$

Statistical analysis

The results obtained were analyzed using a one-way ANOVA test to significantly determine the difference among treatments whose degree of confidence was above 95% ($P < 0.05$).

Results

The photosensitizers (AgNPs) were synthesized by reducing $AgNO_3$ using ($Na_3C_6H_5O_7$). The absorption spectrum of AgNPs was measured using a UV-visible spectrophotometer. The full width at half maximum (FWHM) of the AgNP spectrum is wide, which means the solution has many absorption spectrums (not specifically). In this case, the solution can absorb energy from 360 to 541 nm of wavelength. The absorption peak which occurs at 441 ± 191.2 nm of wavelength was 0.437 ± 0.002 a.u as shown in Fig. 2. However, the laser diode spectrum used as light source of 450 ± 22.34 nm was still in the range spectrum of AgNPs.

PSA was used to determine the distribution size of the synthesized AgNPs. The size of the AgNP distribution has been recorded against the particles number. The sample test was carried out at 25 °C, using an aqueous solvent, a refractive index of 1330, a viscosity degree of 0.8872 cP, and a mean size of 59.19 nm. Figure 3 shows that the particle size of

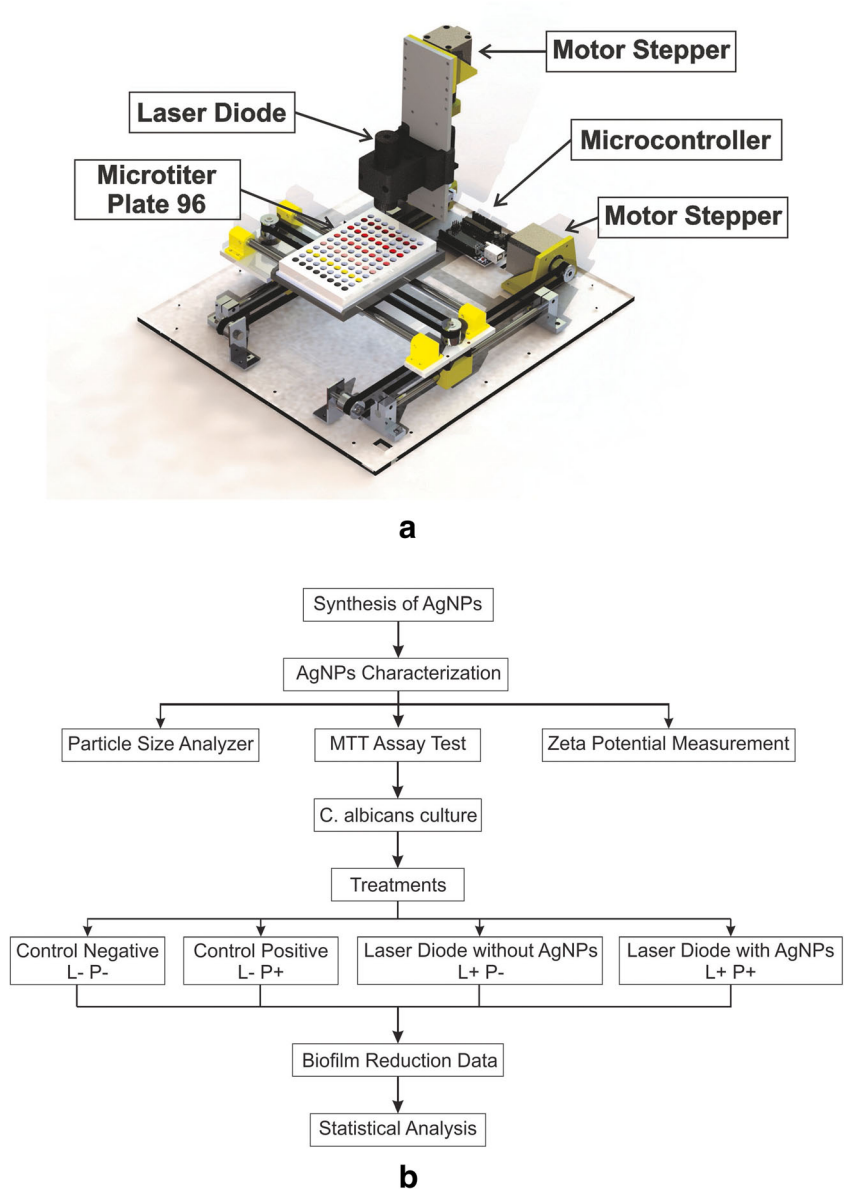

Fig. 1 **a** Representative images of the experimental setup during the laser irradiation process. **b** Flowchart describing the variation of treatment used biofilm of *C. albicans* as a target

Table 1 Sample treatments for reducing biofilm of *C. albicans*

Sample treatments	AgNPs			Laser diode		
	pH	Volume (μL)	Concentration (mM)	Energy density (J/cm^2)	Energy (J)	Time (s)
pH variation	3	100	1	–	–	–
	7	100	1	–	–	–
	9	100	1	–	–	–
	11	100	1	–	–	–
Laser irradiation	–	100	1	6.13	0.8	15
	–	100	1	12.27	1.6	30
	–	100	1	36.80	4.78	90
	–	100	1	122.68	15.95	300
	–	100	1	245.35	31.9	600
	–	100	1	490.71	63.79	1200

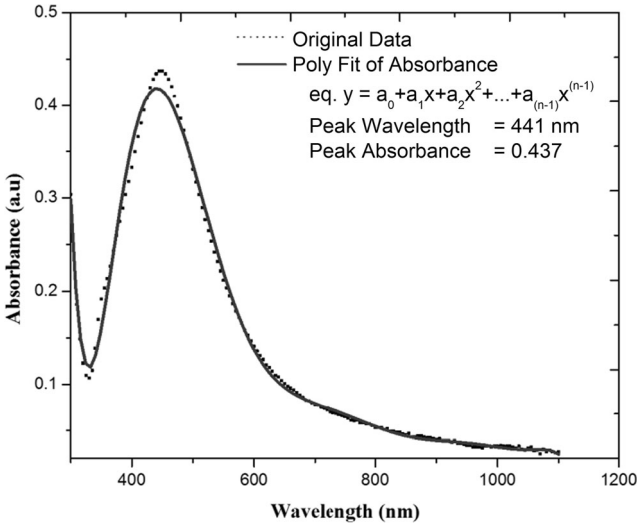

Fig. 2 The absorption spectrum of AgNPs

AgNPs was distributed between 7.531–5559.644 nm with a peak in the range 20–180 nm and PdI value 0.460. The result of calculation by determining the area of each peak was the total distribution of 1797.65 particles with a particle distribution in region I of 29.61 particles; region II has 1725.7 particles and region III has 42.34 particles, then the percentage probability of each area was distributed at 1.64%, 96%, and 2.36%.

The result of cytotoxicity test of AgNPs using human hepatocyte cells indicated that the cell viability in different concentrations (A (1 mM) 72.17%, B (0.05 mM) 71.44%, and C (0.1 mM) 76.97%) was non-cytotoxic. All of the viability cells were above 50% and indicated that the AgNPs used in this study were safe [25]. The stability properties of colloidal AgNP have been tested with different pH conditions against zeta potential in Table 2.

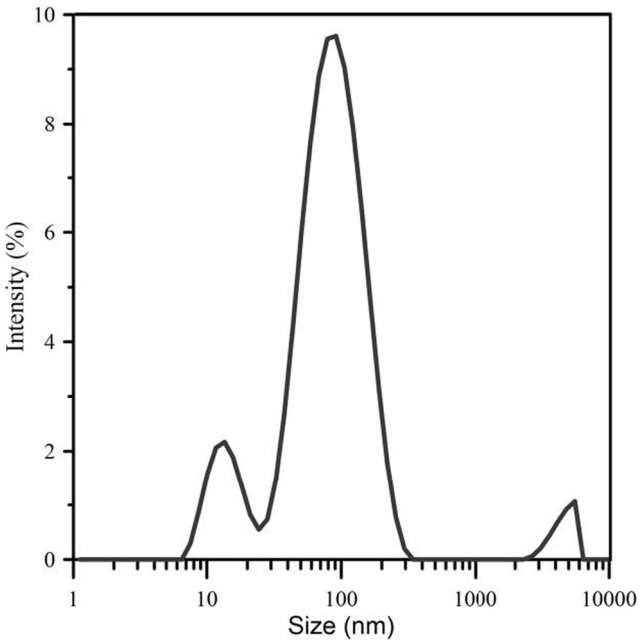

Fig. 3 The distribution nanoparticles size of AgNPs

A zeta potential was used to determine the surface potential of the AgNPs. Measurements of zeta potential were also carried out in order to study the stability of nanoparticles as this extremely important for many applications. The criteria of stability of nanoparticles are measured when the values of zeta potential ranged from higher than + 30 mV to lower than − 30 mV [27]. The pH is the main factor that was affecting the zeta potential value.

Therefore, by using the AgNPs, the pH control plays its role during the treatment. For the obtained nanoparticles, zeta values were measured and found to fall between − 20.53 and − 50.10 mV. The results showed that at pH 3, colloidal AgNPs were unstable with zeta − 20.53 mV due to the addition of the HCl solution, which could decrease the stability of colloidal AgNPs. The clone is absorbed into particles resulting in a decrease in the surface tension as indicated by the low potential zeta value. The AgNPs at pH values 7, 9, and 11 showed stable colloidal AgNPs because the values of zeta potential are lower than − 30 mV. The stability of colloidal AgNPs is due to the presence of charge on the surface of AgNPs. The amount of charge on the surface of AgNPs is influenced by the concentration of electrolyte present in the dispersing medium. After testing, the colloidal AgNPs were applied to increase the *C. albicans* biofilm reduction.

The shape and size of AgNPs was shown in Fig. 4. The AgNPs were in a spherical shape with a size of 10–13 nm which was in the mean particle size. The AgNPs was evenly distributed and even had a smaller size in several points.

The diagram (Fig. 5) shows that a high reduction percentage is caused by different treatments. Sample L + P− was treated with a laser without AgNPs and sample L + P+ treated with a combination of laser with AgNPs. Biofilm reduction (%) without AgNPs was used for the comparison of L + P− with L − P− treatment and biofilm reduction with AgNPs was used for the comparison of L + P+ with L − P+ treatment by using Eq. (1). Laser treatment was carried out at the same range time and the energy density in both samples; thus, results were only the effect of adding AgNPs. The increasing of biofilm reduction caused by increasing of the energy density of both treatments was not significantly different based on the statistical analysis.

Table 2 The results of treatment with AgNPs in various pH

pH	Zeta potential (mV)	Biofilm reduction (%)
3	− 20.53	26.79
7	− 45.63	41.14
9	− 62.00	29.42
11	− 50.10	30.59

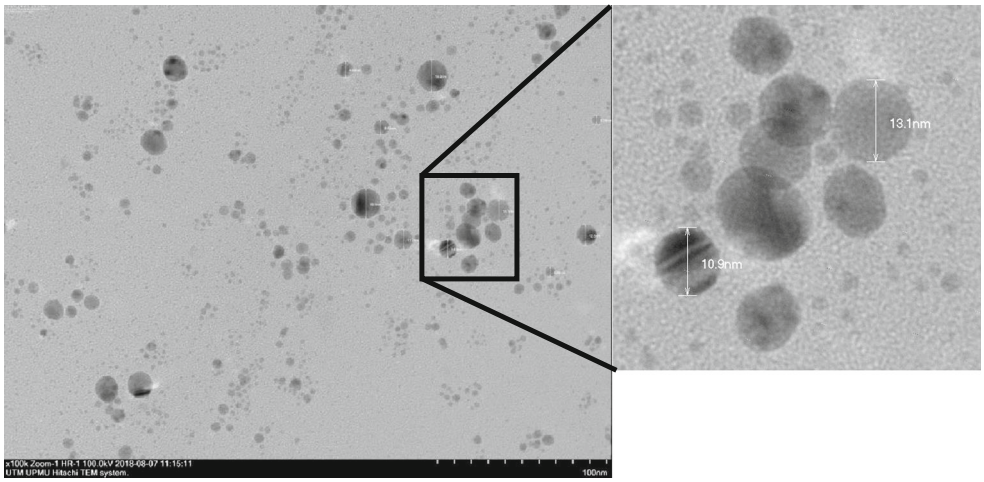

Fig. 4 The TEM image of AgNPs with × 100 magnification

Based on Fig. 5, the treatment with a laser diode as a light source (L + P−) showed an increase of biofilm reduction at 600 s. This result showed that the combination of the laser diode and AgNPs (L + P+) showed a rapid increase in biofilm reduction since the start of irradiation. However, in the statistical analysis, irradiation on 600 s was more effective on both treatments, although exposure of 1200 s gave a higher efficiency level. The difference in biofilm reduction between the two treatments was more noticeable at a low energy density of the laser diode without AgNPs (L + P−) giving a 7.07% biofilm reduction and laser treatment with AgNPs (L + P+) gave a 64.48% biofilm reduction.

Discussion

The stability of the AgNPs was affected by the pH value of solution with Zeta potential. The adjustment of pH value was done to maintain the particles in nanosize (Table 2). The size of AgNPs obtained from TEM image was 10–13 nm in the range of mean size particles based on the PSA result which was 7.531–5559.644 nm. The particles would be diffused into the biofilm and produce a toxic molecule to reduce the biofilm. The diffusion of particles in general depends on the porous structure of the biofilm, the local accumulation of the nanoparticles by cell, the non-diffusing macromolecules or the polysaccharide network, and the adsorption of the solute to freely diffusing species, abiotic particles, or gas bubbles.

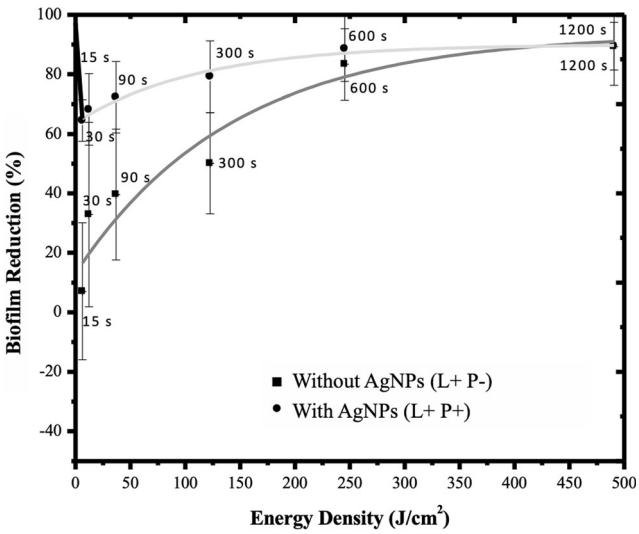

Fig. 5 Reduction percentage of *C. albicans* death cell in various treatments

Based on the result of this study, the biofilm reduction increased with the combination of the laser diode and AgNPs. Compared to the study of Kim et al., they reported that the AgNPs could damage the cell membrane structure and inhibit the normal budding process because of the disintegration of the cell membrane [28]. The other study conducted by Lara et al. also reported that the AgNPs with positive charge could damage the cell membrane. It also could permeate the outer cell wall of bacteria and inhibit the biofilm formation [29]. Both studies showed that AgNPs had an antibacterial effect and antifungal effects. Another study from Silva et al. mentioned that the AgNPs had the antibacterial and antifungal effect by reducing *Candida* biofilm [14]. From all these studies, they used only AgNPs in reducing the biofilm. On the other hand, our study implied that the combination of the laser diode and AgNPs improved the biofilm reduction, especially in *C. albicans*.

In addition to toxic effects resulting from its nature, AgNPs could also be more toxic due to the release of Ag+ ions, which have well-known antibacterial and other destructive agents. It is possible that surface oxidation species on the surface of AgNPs, upon contact with cell culture medium or proteins in the matrix EPS, liberates Ag+ ions that could amplify the toxicity [30]. It is acknowledged and also predicted that due the mechanism when nanoparticles partially diffuse into the biofilm, AgNPs are able to bind with thiol (–SH) species of the proteins

due to its high affinity and affected on changing its original structure and properties (denaturation) [15]. This is of particular concern due to the fact that known thiol groups are one of the functional groups within antioxidants such as glutathione and superoxide dismutase [SOD], which become an important point to the antioxidant defense system for terminating the oxidation reaction that occurs due to the presence of silver ion. Therefore, thiyl radical produced by thiol and the AgNP reaction is very reactive with oxygen, which produces other free radical. AgNPs may deplete cellular antioxidants and accumulate ROS on biofilm (endogenous ROS) [15]. ROS are highly reactive compounds which may bind with biological molecules (such as protein, lipid, and DNA) whereby causing damage. The ROS production in the biofilm that exceeds capacity and ability to remove the protector caused oxidative stress (Fig. 6).

There are three possible mechanisms, namely thiyl radical, light absorption by biofilm, and localized surface plasmon resonance (LSPR) which was shown in Fig. 6. Treatment of the addition of AgNPs causes the formation of free radicals, when in large quantities, would damage the ROS accumulation. Oxidative stress occurs when the amount of ROS formed exceeds the number of protectors produced by the cell. After incubation with AgNPs, samples were irradiated with a laser that allowed the absorption of photons (exogenous ROS) by matrix biofilms and particles of AgNPs. One possibility is that microorganisms sensitive to laser light may have some substance which acts as an endogenous photosensitizer and that the sensitivity may vary according to the level or type of this substance [21]. Furthermore, this possibility leads to produce ROS and accumulated with ROS from other reaction. But this mechanism is still unclear.

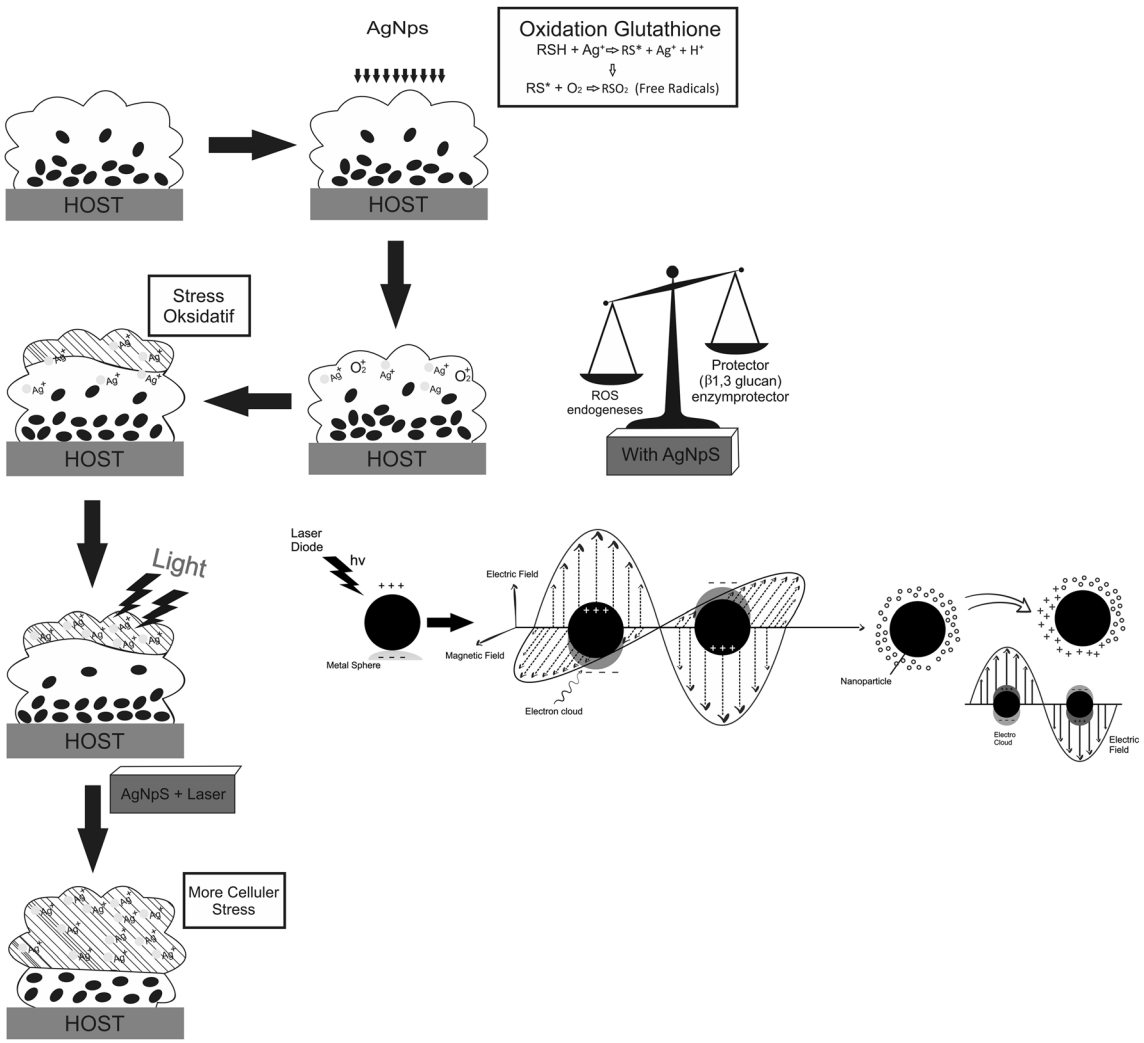

Fig. 6 Schematic mechanism of *C. albicans* biofilm reduced by silver nanoparticles (AgNPs) only and combination with a light source

When particles of AgNPs interact with photons from lasers, it will absorb the energy of laser photons; the electromagnetic fields of the lasers cause the polarization of the conduction band electrons (free electrons) on the surface of the nanoparticles. Because the electromagnetic field of light oscillates, the polarization of the electrons also undergoes oscillation. The heat generation of silver nanoparticles interact with visible light is due to the surface localized plasmon resonance (LSPR) phenomenon, which occurs when the size of nanoparticles is smaller than the wavelength of light. To explain this phenomenon, Mie's theory can be used to quantify the SPR by scattering and absorption of light by small particles in terms of their extinction, scattering, and absorption coefficient. By applying Mie's theory, the heating generation of silver nanoparticles which interact with lasers in our case can be reasonably explained, since the size of the nanoparticle (in the range 20–180 nm) is far smaller than the wavelength used (450 nm).

In general, there are four steps involved in heat generation process: (1) collective free electrons in the surface of silver nanoparticle (plasmon) absorb the energy of photons from laser beam on a time scale of 100 fs; (2) the state of equilibrium distribution is achieved through electron-electron relaxation on the order of 10–100 fs; (3) particle temperature in the surface of silver nanoparticle increases due to electron-phonon coupling effect, happening approximately between 100 fs and 10 ps; (4) temperature rises in surrounding medium through energy exchange between the nanoparticle and their surrounding medium by phonon-phonon coupling on the order of 1 ps to 1 ns [31].

Conclusion

In conclusions, irradiation with a 450nm light source has a significant fungicidal effect on *C. albicans* biofilm. The combination of light source and AgNPs provides an increase of biofilm reduction compared to light source itself. Moreover, it is recommended to use this combination at a low energy density of the light source.

Funding information This work was supported by internal research fund of Postgraduate School Universitas Airlangga, Indonesia, No. 843/UN3.1.15/PPd/2017.

Compliance with ethical standards

Conflict of interest The authors declare they have no conflict of interest.

References

1. Arendrup MC (2011) National surveillance of fungemia in Denmark (2004 to 2009). J Clin Microbiol 49:325–334. https://doi.org/10.1128/JCM.01811-10
2. Martin GS, Mannino DM, Eaton S, Moss M (2003) The epidemiology of sepsis in the United States from 1979 through 2000. N Engl J Med 384:1546–1554. https://doi.org/10.1056/NEJMoa022139
3. Pfaller MA, Moet GJ, Messer SA, Jones RN, Castanheira (2011) *Candida* bloodstream infections: comparison of species distributions and antifungal resistance patterns in community-onset and nosocomial isolates in the SENTRY antimicrobial surveillance program, 2008–2009. Antimicrob Agents Chemother 55(2):561–566. https://doi.org/10.1128/AAC.01079-10
4. Hermsen DE, Zapapas MK, Maiefski M, Rupp ME, Freifeld AG, Kalil AC (2011) Validation and comparison of clinical prediction rules for invasive candidiasis in intensive care unit patients: a matched case-control study. Crit Care 15:1–8. https://doi.org/10.1186/cc10366
5. Pu S (2017) Epidemiology, antifungal susceptibilities and risk factors for invasive candidiasis form 2011 to 2013 in a teaching hospital in southwest China. J Microbiol Immunol Infect 50:97–103. https://doi.org/10.1016/j.jmii.2015.01.005
6. Yapar N (2014) Epidemiology and risk factors for invasive candidiasis. Ther Clin Risk Manag 10:95–105. https://doi.org/10.2147/TCRM.S40160
7. Baillie GS (2000) Matrix polymers of Candida biofilm and their possible role in biofilm resistance to antifungal agents. J Antimicrob Chemother 46:397–403
8. Ramage G, Saville SP, Thomas DP (2005) Candida biofilm: an update. Eukaryotic Cell (4) 4:633–663. https://doi.org/10.1128/EC.4.4.633-638.2005
9. Sheppard DC, Howell PL (2016) Biofilm exopolysaccharides of pathogenic fungi: lesson from bacteria. J Biol Chem 291:12529–12537. https://doi.org/10.1074/jbc.R116.720995
10. Udapudi B, Naik P, Savadatti SP, Sharma R, Samprita B (2012) Synthesis and characterization of silver nanoparticles. Int J Pharm Biol Sci 2:10–14
11. Rahisuddin TSA, Khan Z, Manzoor N (2015) Biosynthesis of silver nanoparticles and its antibacterial and antifungal activities towards Gram-positive, Gram-negative bacterial strains and different species of Candida fungus. Bioprocess Biosyst Eng. https://doi.org/10.1007/s00449-015-1418-3
12. Monteiro DR, Negri M, Silva S, Gorup LF, Camargo ER, Oliveira R, Barbosa DB, Henriques M (2014) Adhesion of Candida biofilm cells to human epithelial cells and polystyrene after treatment with silver nanoparticles. Lett Colloids and Surfaces B: Biointerfaces 114:410–412. https://doi.org/10.1016/j.colsurfb.2013.10.027
13. Monteiro DR (2012) Silver nanoparticles: influence of stabilizing agent and diameter on antifungal activity against Candida albicans and Candida glabrata biofilms. Lett Appl Microbiol 54:383–391. https://doi.org/10.1111/j.1472-765X.2012.03219.x
14. Silva S, Pires P, Monteiro DR, Negri M, Gorup LF, Camargo ER, Barbosa DB, Oliveira R, Williams DW, Henriques M, Azeredo J (2012) The effect of silver nanoparticles and nystatin on mixed biofilms of *Candida glabrata* and *Candida albicans* on acrylic. Med Mycol Month. https://doi.org/10.3109/13693786.2012.700492
15. Jhonston HJ, Hutchison G, Christensen FM, Peters S, Hankin S, Stone V (2010) A review of the in vivo and in vitro toxicity of silver and gold particulates: particle attributes and biological mechanisms responsible for the observed toxicity. Crit Rev Toxicol 40:328–346. https://doi.org/10.3109/10408440903453074

16. Souza RC, Junqueira JC, Rossoni RD, Pereira CA, Munin E, Jorge AOC (2010) Comparison of the photodynamic fungicidal efficacy of methylene blue, toluidine blue, malachite green and low-power laser irradiation alone against Candida albicans. Lasers Med Sci 25: 385–389. https://doi.org/10.1007/s10103-009-0706-z
17. Choi HA (2017) Antimicrobial and anti-biofilm activities of the methanol extracts of medicinal plants against dental pathogens Streptococcus mutans and Candida albicans. J Microbiol Biotechnol 27:1242–1248. https://doi.org/10.4014/jmb.1701.01026
18. Raut JS, Shinde RB, Chauhan NM, Karuppayil SM (2017) Activity of allyl isothiocyanate and its synergy with fluconazole against *Candida albicans* biofilm. J Microbiol Biotechnol 27:685–693. https://doi.org/10.4014/jmb.1607.07072
19. Astuti SD, Arifianto D, Drantantyas NDG, Nasution AMT, Abdurachman (2016) Efficacy of CNC-diode laser combined with chlorophylls to eliminate *Staphylococcus aureus* biofilm. Int Semin Sensors Instrum Meas Metrol. https://doi.org/10.1109/ISSIMM.2016.7803722
20. Peulen TO, Wilkinson KJ (2011) Diffusion of nanoparticles in a biofilm. Environ Sci Technol 45:3367–3373. https://doi.org/10.1021/es103450g
21. Imamura T, Tatehara S, Takebe Y, Tokuyama R, Ohshima T, Maeda N, Satomura K (2014) Antibacterial and antifungal effect of 405 nm monochromatic laser on endodontopathogenic microorganisms. Int J Photoenergy 1:1–7. https://doi.org/10.1155/2014/387215
22. Siems A, Weber SAL, Boneberg J, Plech A (2011) Thermodynamics of nanosecond nanobubble formation at laser-excited metal nanoparticles. New J Phys 13:043018. https://doi.org/10.1088/1367-2630/13/4/043018
23. Kojic N, Pritchard EM, Tao H, Brenckle MA, Mondia JP, Panilaitis B, Omenetto F, Kaplan DL (2012) Focal infection treatment using laser-mediated heating of injectable silk hydrogels with gold nanoparticles. Adv Funct Mater 22(18):3793–3798. https://doi.org/10.1002/adfm.201200382
24. Rashid MU, Md. Bhuiyan KH, Quayum ME (2013) Synthesis of silver nano particles (Ag-NPs) and their uses for quantitative analysis of vitamin C tablets. Dhaka Univ J Pharm Sci 12(1):29–33. https://doi.org/10.3329/dujps.v12i1.16297
25. Kawata K, Osawa M, Okabe S (2009) In vitro toxicity of silver nanoparticles at non-cytotoxic doses to HepG2 human hepatoma cells. Environ Sci Technol 43:6046–6051. https://doi.org/10.1021/es900754q
26. Dhale RP, Ghorpade MV, Dharmadhikari (2014) Comparison of various methods used to detect biofilm production of Candida species. J Clin Diagnostic Res 8(11):18–20. https://doi.org/10.7860/JCDR/2014/10445.5147
27. Prathna TC, Chandrasekaran N, Raichur AM, Mukherjee A (2011) Biomimetic synthesis of silver nanoparticles by *Citrus limon* (lemon) aqueous extract and theoretical prediction of particle size. Colloids Surf B Biointerfaces 82(1):152–159. https://doi.org/10.1016/j.colsurfb.2010.08.036
28. Kim KJ, Sung WS, Suh BK, Moon SK, Choi JS, Kim JG, Lee DG (2009) Antifungal activity and mode of action of silver nanoparticles on *Candida albicans*. Biometals 22:235–242. https://doi.org/10.1007/s10534-008-9159-2
29. Lara HH, Romero-Urbina DG, Pierce C, Lopez-Ribot JL, Arellano-Jimenez MJ, Jose-Yacaman M (2015) Effect of silver nanoparticles on *Candida albicans* biofilms: an ultrastructural study. J Nanobiotechnol 13(91). https://doi.org/10.1186/s12951-015-0147-8
30. Zhang R (2012) Endoplasmic reticulum stress signaling is involved in silver nanoparticles-induced apoptosis. Int J Biochem Cell Biol 44:224–232. https://doi.org/10.1016/j.biocel.2011.10.019
31. Liu X, Shan G, Yu J, Yang W, Ren Z, Wang X, Xie X, Chen H-J, Chen X (2017) Laser heating of metallic nanoparticles for photothermal ablation applications. AIP Adv 7:2. https://doi.org/10.1063/1.4977554